finger- and nail abnormalities such as camptodactyly and deepset nails (**Cole et al., 1992; Opitz et al., 1998; Proud et al., 1998**). Due to the phenotypic overlap, distinction between Weaver and Sotos syndrome can be difficult (see further).

MOLECULAR GENETICS

Spectrum of *NSD1* Abnormalities in Sotos Syndrome

In 2002, a de novo balanced reciprocal translocation, 46,XX,t(5;8)(q35;q24.1), was described in a Japanese infant with Sotos syndrome (**Imaizumi et al., 2002**). Subsequently, the location of the breakpoint was mapped to 5q35.2-q35.3, disrupting the *NSD1* gene (**Kurotaki et al., 2002**). Within a Sotos syndrome group consisting of 42 Japanese individuals, four different de novo point mutations and 20 submicroscopic deletion mutations of *NSD1* were found (**Kurotaki et al., 2002**). Since then, several reports (see Table 113–1 and references) have shown that intragenic point mutations of *NSD1* are the main cause of Sotos syndrome in non-Japanese populations and that microdeletions of the whole *NSD1* gene account for nearly 10% of the cases. In contrast, these microdeletions are the major cause of Sotos syndrome in the Japanese populations, with point mutations only occurring in approximately 10%.

Although mutations resulting in protein truncation are found throughout the *NSD1* gene without specific hotspot locations, missense mutations are preferentially located in the functional domains of *NSD1* (see Fig. 113–1).

In addition, intragenic partial microdeletions of *NSD1*, comprising a single or multiple exons, were reported in 8 out of 124 individuals (6%) with a classic Sotos syndrome phenotype (**Douglas et al., 2005b**). Remaining causes of *NSD1* abnormalities could be intronic mutations affecting splicing or changes in the regulatory factors controlling the expression of *NSD1*, which cannot be detected with the present techniques. Despite the high detection rate (90%–93%) of *NSD1* abnormalities in certain studies (**Turkmen et al., 2003; Tatton-Brown et al., 2005b**), also genetic locus heterogeneity cannot be excluded totally. A recent study did not detect any sequence abnormalities or epigenetic changes of the *NSD1* promoter region in a group of 18 classical Sotos syndrome patients without any confirmed *NSD1* sequence abnormalities or gene deletions (**Visser et al., 2006**).

NSD1 Abnormalities in Other Overgrowth Syndromes

To date, only six Weaver syndrome patients have been described harboring an intragenic *NSD1* point mutation (**Douglas et al., 2003; Rio et al., 2003**) and the screening was negative in 16 additional patients (**Douglas et al., 2003; Rio et al., 2003; Turkmen et al., 2003; Cecconi et al., 2005; Tong et al., 2005**). Furthermore, the three patients from **Douglas et al. (2003)** initially described as Weaver syndrome were reclassified as typical Sotos (2) and Sotos-like (1) in a recent study (**Tatton-Brown et al., 2005b**). Therefore, it remains questionable whether *NSD1* abnormalities are responsible for classic Weaver syndrome, as is also noted by others (**Tatton-Brown et al., 2005b**).

Recently, two patients with Beckwith–Wiedemann syndrome (see Chapter 104) were reported to carry *NSD1* mutations (**Baujat et al., 2004**). Furthermore, a Japanese patient with Nevo syndrome and a submicroscopic deletion of *NSD1* was reported (**Kanemoto et al., 2006**). Additional patients are necessary to determine whether these cases are accidental (due to an overlap phenotype) or whether a small subgroup of these syndromes is caused by an *NSD1* abnormality.

NSD1 abnormalities were not detected in a large group of patients with a nonspecific overgrowth phenotype (**Douglas et al., 2003; Turkmen et al., 2003; Cecconi et al., 2005**). Because of the large number of patients screened to date, including populations with a broad range of phenotypes, it can be reasonably concluded that *NSD1* abnormalities are specific to Sotos syndrome.

Other Causes of Sotos Syndrome

In two patients with a Sotos syndrome phenotype, abnormalities were detected in the imprinted region on 11p15, which is associated with Beckwith–Wiedemann syndrome (**Baujat et al., 2004**). Although additional patients have yet to be reported, it is interesting to hypothesize that the histone methyltransferase activity of NSD1 could be a factor playing a role in establishing the parental imprint in this region (**Baujat et al., 2004**).

In 78 Sotos patients in whom *NSD1* abnormalities were excluded, the *NSD*-gene–family members *NSD2* and *NSD3* were screened but no mutations were found (**Douglas et al., 2005a**).

Mechanism of Submicroscopic Microdeletions of *NSD1*

The studies in the Japanese Sotos syndrome patients showed a high frequency of common approximately 2.2 Mb microdeletions, including *NSD1* and neighboring genes (**Kurotaki et al., 2002; Kurotaki et al., 2003**). The breakpoints occurred in flanking highly homologous genomic segments, so-called low-copy-repeats (LCRs) (**Kurotaki et al., 2003**). In six out of eight investigated cases, the meiotic rearrangement was of intrachromosomal origin and a preference was found for the paternally derived chromosome (18/20) (**Miyake et al., 2003**).

Table 113–1. Frequency of *NSD1* Mutations and Microdeletions in Sotos Syndrome[a]

Study	*NSD1* Abnormalities (%)	Intragenic Mutations (%)	Microdeletions (%)
Kurotaki et al., 2002	57 (24/42)	10 (4/42)	48 (20/42)
Douglas et al., 2003	64 (32/50)	58 (29/50)	6 (3/50)
Kamimura et al., 2003[†]	27 (8/30)	27 (8/30)	
Rio et al., 2003	67 (22/33)	48 (16/33)	18 (6/33)
Türkmen et al., 2003[‡]	90 (19/21)	90 (19/21)	0
Kurotaki et al., 2003[b,c]	59 (66/112)	14 (16/112)	45 (50/112)
Melchior et al., 2004	33 (11/33)	27 (9/33)	6 (2/33)
de Boer et al., 2004b[‡]	43 (23/53)	36 (19/53)	8 (4/53)
Cecconi et al., 2005	52 (17/33)	48 (16/33)	3 (1/33)
Tong et al., 2005	72 (26/36)	64 (23/36)	8 (3/36)
Waggoner et al., 2005[††]	13 (55/435)	21 (46/217)	2 (9/378)
Tatton-Brown et al., 2005b[‡‡]	93 (115/124)	77 (96/124)	10 (12/124)[***]

[a]No distinction is made between "classical" Sotos syndrome and "Sotos-like."
[b]Microdeletions were excluded before screening.
[c]Familial cases are counted as one single mutation and only one patient per family is included.
[**]There is an overlap with the patient population from **Kurotaki et al., 2002**.
[††]Both *NSD1* mutation and deletion analyses were not performed in all patients.
[‡‡]From this study only the subjects from the United Kingdom are shown in order to exclude overlap with previous studies. There is a remaining overlap with the patient population from **Douglas et al., 2003**.
[***]Partial-gene deletions 6% (7/124) are not included.

The flanking LCRs were analyzed to have a high overall sequence similarity of approximately 98.5% and to be in an inverted orientation, except for an approximately 51 kb directly orientated region (see Fig. 113–3) (**Visser et al., 2005b**). The deletion breakpoints were mapped in approximately 79% (37/47) of a group of Japanese Sotos syndrome patients to a 3.0 kb recombination hotspot and the deletion size was refined to 1.9 Mb (**Visser et al., 2005b**). In another study, four additional deletion breakpoints were localized inside the directly orientated regions, but outside the Sotos recombination hotspot (**Visser et al., 2005a**). Nonallelic homologous recombination between the directly orientated regions (PLCR-B and DLCR-2B) was determined to be the underlying mechanism of the microdeletions (**Kurotaki et al., 2005a; Visser et al., 2005b**).

In a group of non-Japanese Sotos syndrome patients with a microdeletion size varying from 0.4 to 5.0 Mb, rearrangement occurred through an interchromosomal mechanism preferentially in the paternally derived chromosome (**Tatton-Brown et al., 2005a**). In contrast to the Japanese Sotos syndrome population, the detected microdeletion could have been mediated by the flanking Sotos LCRs in only 55% (18/33). For the remaining 45% (15/33), a microdeletion-causing mechanism differing from that in the Japanese population is likely (**Tatton-Brown et al., 2005a; Visser et al., 2005b**).

Since the Sotos syndrome LCRs are present in both the Japanese and non-Japanese population, it can be hypothesized that a specific genomic variation increases susceptibility for microdeletions in the Japanese population. A heterozygous inversion of the genomic interval between the Sotos LCRs was found in the parents [mothers 85% (11/13); fathers 100% (18/18)] of the Sotos patients carrying a microdeletion and also in a small Japanese control population [female 75% (3/4); male 67% (4/6)]. This inversion might interfere with meiotic pairing and consequently predispose to nonallelic homologous recombination (**Visser et al., 2005b**). However, further studies in Sotos syndrome and normal populations of different ancestry are necessary for elucidation of the prevalence and the role of this possible genomic inversion polymorphism.

Genotype–Phenotype Correlation in *NSD1* Abnormalities

In genotype–phenotype correlations in Sotos syndrome, an interesting point is whether Sotos characteristics are specifically attributable to *NSD1* abnormalities or whether neighboring dose-sensitive genes in the deleted segment contribute to additional features in Sotos syndrome. In an initial study consisting of five individuals harboring point mutations and 21 patients with a microdeletion, it was suggested that patients with a microdeletion showed a tendency to have smaller height and a more severe level of retardation than those with an intragenic mutation (**Nagai et al., 2003**). These results were confirmed in a study group comprised of 31 microdeletions and 208 intragenic mutations, which showed a significant difference for less-prominent overgrowth and more severe learning disability in the patients carrying microdeletions (**Tatton-Brown et al., 2005b**). The study by **Nagai et al. (2003)** also showed that some major anomalies in the central nervous, cardiovascular, and genitourinary system were only present in the microdeletion group. Although no significant difference in the prevalence of anomalies was found, a tendency toward more cardiac anomalies in the microdeletion group was observed by **Tatton-Brown et al. (2005b)**. In addition, there were no differences in associated features in relation to the different deletion sizes (**Tatton-Brown et al., 2005b**). A recent study showed that the plasma activity of coagulation factor 12 (FXII; also known as Hageman factor) in Sotos syndrome patients carrying a common deletion comprising *NSD1* and the *FXII* gene was correlated with a functional polymorphism of the nondeleted hemizygous *FXII* allele (**Kurotaki et al., 2005b**). Although the significance of the low level of FXII plasma

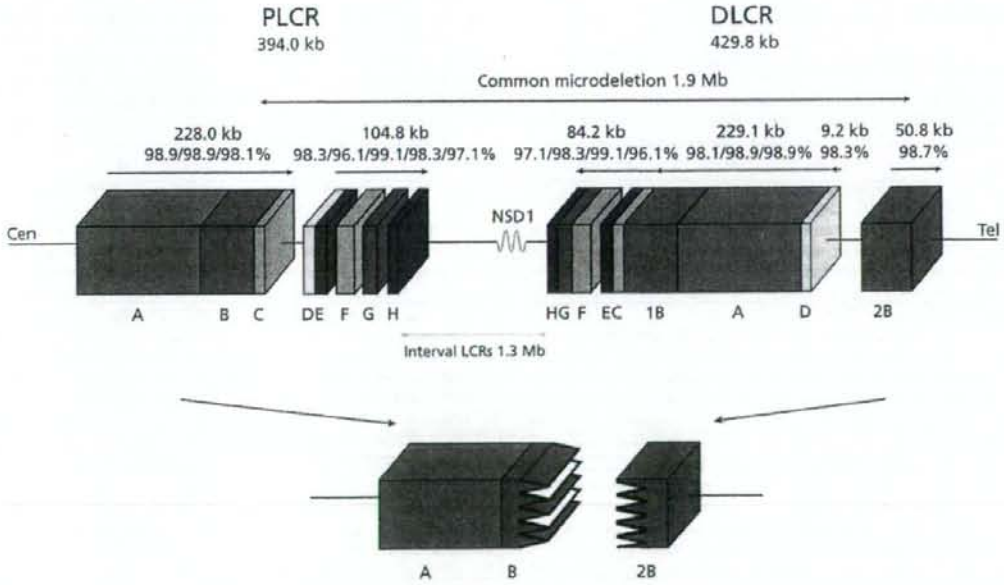

Figure 113–3. Schematic presentation of the two low copy repeats (LCRs) harboring the breakpoints of the common 1.9 Mb microdeletion in Sotos syndrome. In the lower part of the figure, the most common recombination (between PLCR-B and DLCR-2B) is shown. Blocks with the same color and same letter written below depict regions with sequence homology to each other. The size of (groups of) blocks and the sequence identity percentages are shown above the blocks. The direction of the horizontal arrows indicates the genomic orientation. The interval that might be involved in a predisposing inversion polymorphism (see text) is shown with an orange bidirectional arrow below the LCRs. (Fig. 113–3 is a modified version of Figure 1 from **Visser et al., 2005b** with kind permission from The University of Chicago Press, copyrights 2004 by The American Society of Human Genetics. All rights reserved.)

activity is yet unknown, its clinical consequences are considered to be small (**Kurotaki et al., 2005b**).

Since haploinsufficiency of the deleted genes in the microdeletion region has not been associated with specific additional features yet, it can be concluded that the Sotos phenotype is primarily caused by a reduced level of proper functioning NSD1.

DIAGNOSIS OF SOTOS SYNDROME

Nowadays, the diagnosis of Sotos syndrome is established by confirmation of *NSD1* abnormalities in patients with a phenotypical Sotos syndrome or with some Sotos syndrome characteristics. Analysis of *NSD1* includes at least the sequence analysis of exon 2–23 including exon–intron boundaries and either multiplex ligation probe amplification (MLPA) or fluorescent in situ hybridization (FISH) for possible deletions. MLPA is the preferred method for detection of intragenic and whole-gene deletions (**Douglas et al., 2005b**), while FISH analysis can be used for whole-gene deletions and investigation of the size of the broader deleted region (**Kurotaki et al., 2003**).

Because *NSD1* testing is now commonly available, physicians facing suspected patients should maintain a low threshold for *NSD1* testing. However, it is important to emphasize the importance of a good clinical diagnosis as the detection rate in a referral laboratory is significantly lower (13%) (**Waggoner et al., 2005**) compared to that in strictly diagnosed patient groups (90%–93%) (**Turkmen et al., 2003; Tatton-Brown et al., 2005b**).

Furthermore, screening of overgrowth patients without Sotos phenotypic features has not yet identified *NSD1* abnormalities (**Turkmen et al., 2003; Cecconi et al., 2005; Tatton-Brown et al., 2005b**). Therefore, standard screening of patients with a nonspecific overgrowth phenotype cannot be substantiated with the present literature. For patients with an overlapping phenotype of Beckwith–Wiedemann and Sotos syndromes, it is advisable to investigate both *NSD1* as well as 11p15 abnormalities (**Baujat et al., 2004**).

Although *NSD1* is not likely to be the causative gene of the classic Weaver syndrome, testing of *NSD1* is advised because the phenotypic differentiation from Sotos syndrome can be difficult. A negative result could also be used as an extra argument in favor of a classic Weaver syndrome diagnosis (**Tatton-Brown et al., 2005b**).

COUNSELING AND MANAGEMENT

Sotos syndrome is an autosomal dominant disorder with full penetrance (**Tatton-Brown et al., 2005b**). Therefore, the risk of vertical transmission is 50% when one of the parents is affected. However, most *NSD1* mutations occur de novo. The number of familial cases is lower than expected, suggesting a possible reduced fertility in Sotos patients (**Tatton-Brown et al., 2005b**). Missense mutations located outside the SET domain might be more common in familial mutations, although affected families with truncating mutations have also been reported (**Hoglund et al., 2003; Tatton-Brown et al., 2005b; Tong et al., 2005; Waggoner et al., 2005**). To date, no familial case has been described harboring an *NSD1* deletion.

At present, there is no specific treatment for the *NSD1* gene and protein defect in Sotos syndrome. Therefore, treatment is focused on the management of its manifestations. A large number of associated anomalies have been reported in Sotos syndrome patients (see earlier text), which require specific attention during anamnesis, physical examination, and additional investigations. Especially, at least possible cardiac (amongst others, atrial and ventricle septum defects) and urinary tract anomalies (e.g., vesicoureteral reflux and renal abnormalities) as well as musculoskeletal (for instance, scoliosis and pes planus) problems should be excluded. The incidence of tumors in Sotos syndrome is low (~2%), with a very low risk of malignant transformation (**Rahman, 2005**). Hence, no specific screening targeting tumors in Sotos syndrome other than normal examination seems necessary.

Learning impairment is one of the major criteria of Sotos syndrome and although not validated with *NSD1* analysis, behavior problems in general seem more frequent (**Sarimski, 2003**). Due to the large interindividual variation, it is important for the parents and caretakers to provide a proper (educational) environment for their child with an individualized approach.

MOUSE MODELS

In mice, *Nsd1* expression was seen at various developmental stages, with a ubiquitous expression pattern in both embryonic and extraembryonic tissue till embryonic day 14.5 (**Rayasam et al., 2003**). Subsequently, differential expression was observed in the telencephalic region of the brain, spinal cord, intestinal tooth buds, thymus, salivary glands, in the region of ossification of the developing bones, and in the periosteum (**Rayasam et al., 2003**). Heterozygous targeted $Nsd1^{+/-}$ mice did not to exhibit an apparent Sotos syndrome phenotype, although longer observation periods might be necessary for detection of subtle features (**Rayasam et al., 2003**). The lack of expression of *Nsd1* in mouse chondrocytes observed by **Rayasam et al.** might be an explanation for the lack of overgrowth in mice. Homozygous $Nsd1^{-/-}$ knockout mice died in utero before embryonic day 10.5. In these mutants, an abnormal gastrulation process was noted and Nsd1 is, therefore, thought to be crucial for early postimplantation development (**Rayasam et al., 2003**).

DEVELOPMENTAL PATHOGENESIS

Although the developmental pathogenesis in Sotos syndrome is not yet known, some lines of evidence suggest that NSD1 is associated with transcriptional regulation: first, the capacity to specifically methylate H3-K36 and H4-K20 and second, the interaction with Nizp1, which was shown to be a transcriptional repressor. Therefore, it is intriguing to hypothesize that haploinsufficiency of *NSD1* would result in the loss of transcriptional silencing of yet unknown growth promoting genes and consequently result in accelerated growth. It is presumed that NSD1 is influencing early stages of development since expression is found both in human fetal tissues as well as in mouse embryonic tissues, with Nsd1 being essential for early postimplantation development in mice (**Kurotaki et al., 2001; Rayasam et al., 2003**). In regard to these early expression patterns, overgrowth features and the facial gestalt can already be observed at birth, although the accelerated growth pattern and facial features are usually more pronounced in the early childhood. Considering the developmental delay in Sotos syndrome patients and a high prevalence (without confirmed *NSD1* analyses) of intracranial manifestations, such as enlarged ventricles, prominent trigone, and midline abnormalities (**Schaefer et al., 1997**), the normal neural development is likely to be affected.

How does an abrogated NSD1 function during the different stages of development result in the Sotos syndrome phenotype? One approach could be to construct a detailed phenotype–genotype correlation. However, such analysis would need a significant number of patients in combination with extensive clinical evaluation in order to also detect subtle differences. In general, no difference in phenotype–genotype correlation has been found so far between missense mutations and nonsense mutations in Sotos syndrome (**Tatton-Brown et al., 2005b**). Furthermore, different features were also found in patients with identical mutations (**Tatton-Brown et al., 2005b**). Mutations in familial cases are positioned outside the SET domain, implying a possible relationship of this domain with fertility (**Tatton-Brown et al., 2005b**). Although (because of this?) there are only about 25 familial cases to substantiate this observation (**Hoglund et al., 2003; Turkmen et al., 2003; de Boer et al., 2004b; Tatton-Brown et al., 2005b; Tong et al., 2005; van Haelst et al., 2005; Waggoner et al., 2005; Tei et al., 2006**). In submicroscopic microdeletions including *NSD1* and other genes, the net effect of phenotypic features seems to be attributable to the *NSD1* defect. In summary, the current data regarding the phenotype–genotype correlation are not sufficient to answer the questions related to the Sotos pathogenic pathway.

Establishing the functional network and protein interactions of NSD1 are more likely to create link between genetic abnormalities and the exhibited phenotype, and will yield insight in the underlying pathogenic mechanisms. So far, only Nizp1 has been identified as an interacting protein with NSD1. In addition, NSD1 is thought to act as a cofactor to nuclear hormone receptors in either a ligand dependent or

independent manner. The actual roles of these interactions in relation to the Sotos phenotype continue to be elusive. Identification of more upstream regulators and downstream effectors is necessary in order to be able to map NSD1 into a network of signaling pathways resulting in Sotos syndrome.

CONCLUSION

With the discovery of aberrations of the *NSD1* gene being responsible for Sotos syndrome, research focused on Sotos syndrome has made significant progress in increasing our understanding about the genetic background, the underlying mechanisms of the different *NSD1* abnormalities, and the genotype–phenotype relation. Only limited progress has been made in increasing insight into the possible functions of NSD1. A challenging task for future research projects will be the detailed analyses of these functional roles, identification of NSD1 targets, and unraveling of the signaling pathways in which NSD1 exerts its function(s).

ACKNOWLEDGMENTS

We are very grateful to the patients and parents for their permission to publish the photographs and to their physicians (Dr. S.G. Kant at the Department of Clinical Genetics, Leiden University Medical Center, Leiden, The Netherlands; Dr. N. Okamoto at the Department of Planning and Research, Osaka Medical Center and Research Institute for Maternal and Child Health, Izumi, Japan; and Dr. Y. Makita at the Department of Pediatrics, Asahikawa Medical College, Asahikawa, Japan) for their kind cooperation. R. Visser is supported by grant number 920-03-325 from The Netherlands Organization for Health Research and Development. His Sotos research is financially supported by Stinafo (Stichting Nationaal Fonds "Het Gehandicapte Kind").

References

Aasland R, et al. (1995). The PHD finger: implications for chromatin-mediated transcriptional regulation. *Trends Biochem Sci* 20(2): 56–59.

Angrand PO, et al. (2001). NSD3, a new SET domain-containing gene, maps to 8p12 and is amplified in human breast cancer cell lines. *Genomics* 74(1): 79–88.

Baujat G, et al. (2004). Paradoxical NSD1 mutations in Beckwith-Wiedemann syndrome and 11p15 anomalies in Sotos syndrome. *Am J Hum Genet* 74(4): 715–720.

Cecconi M, et al. (2005). Mutation analysis of the NSD1 gene in a group of 59 patients with congenital overgrowth. *Am J Med Genet A* 134(3): 247–253.

Cole TR, et al. (1992). Weaver syndrome. *J Med Genet* 29(5): 332–337.

Cole TR, Hughes HE (1994). Sotos syndrome: a study of the diagnostic criteria and natural history. *J Med Genet* 31(1): 20–32.

de Boer L, et al. (2004a). Mutations in the NSD1 gene in patients with Sotos syndrome associate with endocrine and paracrine alterations in the IGF system. *Eur J Endocrinol* 151(3): 333–341.

de Boer L, et al. (2004b). Genotype-phenotype correlation in patients suspected of having Sotos syndrome. *Horm Res* 62(4): 197–207.

Douglas J, et al. (2003). NSD1 mutations are the major cause of Sotos syndrome and occur in some cases of Weaver syndrome but are rare in other overgrowth phenotypes. *Am J Hum Genet* 72(1): 132–143.

Douglas J, et al. (2005a). Evaluation of NSD2 and NSD3 in overgrowth syndromes. *Eur J Hum Genet* 13(2): 150–153.

Douglas J, et al. (2005b). Partial NSD1 deletions cause 5% of Sotos syndrome and are readily identifiable by multiplex ligation dependent probe amplification. *J Med Genet* 42(9): e56.

Hoglund P, et al. (2003). Familial Sotos syndrome is caused by a novel 1 bp deletion of the NSD1 gene. *J Med Genet* 40(1): 51–54.

Huang N, et al. (1998). Two distinct nuclear receptor interaction domains in NSD1, a novel SET protein that exhibits characteristics of both corepressors and coactivators. *EMBO J* 17(12): 3398–3412.

Imaizumi K, et al. (2002). Sotos syndrome associated with a de novo balanced reciprocal translocation t(5;8)(q35;q24.1). *Am J Med Genet* 107(1): 58–60.

Jaju RJ, et al. (2001). A novel gene, NSD1, is fused to NUP98 in the t(5;11)(q35;p15.5) in de novo childhood acute myeloid leukemia. *Blood* 98(4): 1264–1267.

Kanemoto N, et al. (2006). Nevo syndrome with an NSD1 deletion: a variant of Sotos syndrome? *Am J Med Genet A* 140(1): 70–73.

Kouzarides T (2002). Histone methylation in transcriptional control. *Curr Opin Genet Dev* 12(2): 198–209.

Kurotaki N, et al. (2001). Molecular characterization of NSD1, a human homologue of the mouse Nsd1 gene. *Gene* 279(2): 197–204.

Kurotaki N, et al. (2002). Haploinsufficiency of NSD1 causes Sotos syndrome. *Nat Genet* 30(4): 365–366.

Kurotaki N, et al. (2003). Fifty microdeletions among 112 cases of Sotos syndrome: low copy repeats possibly mediate the common deletion. *Hum Mutat* 22(5): 378–387.

Kurotaki N, et al. (2005a). Sotos syndrome common deletion is mediated by directly oriented subunits within inverted Sos-REP low-copy repeats. *Hum Mol Genet* 14(4): 535–542.

Kurotaki N, et al. (2005b). Phenotypic consequences of genetic variation at hemizygous alleles: Sotos syndrome is a contiguous gene syndrome incorporating coagulation factor twelve (FXII) deficiency. *Genet Med* 7(7): 479–483.

Melchior L, et al. (2005). dHPLC screening of the NSD1 gene identifies nine novel mutations—summary of the first 100 Sotos syndrome mutations. *Ann Hum Genet* 69(Pt 2): 222–226.

Miyake N, et al. (2003). Preferential paternal origin of microdeletions caused by prezygotic chromosome or chromatid rearrangements in Sotos syndrome. *Am J Hum Genet* 72(5): 1331–1337.

Nagai T, et al. (2003). Sotos syndrome and haploinsufficiency of NSD1: clinical features of intragenic mutations and submicroscopic deletions. *J Med Genet* 40(4): 285–289.

Nielsen AL, et al. (2004). Nizp1, a novel multitype zinc finger protein that interacts with the NSD1 histone lysine methyltransferase through a unique C2HR motif. *Mol Cell Biol* 24(12): 5184–5196.

Opitz JM, et al. (1998). The syndromes of Sotos and Weaver: reports and review. *Am J Med Genet* 79(4): 294–304.

Proud VK, et al. (1998). Weaver syndrome: autosomal dominant inheritance of the disorder. *Am J Med Genet* 79(4): 305–310.

Rahman N (2005). Mechanisms predisposing to childhood overgrowth and cancer. *Curr Opin Genet Dev* 15(3): 227–233.

Rayasam GV, et al. (2003). NSD1 is essential for early post-implantation development and has a catalytically active SET domain. *EMBO J* 22(12): 3153–3163.

Rio M, et al. (2003). Spectrum of NSD1 mutations in Sotos and Weaver syndromes. *J Med Genet* 40(6): 436–440.

Rosati R, et al. (2002). NUP98 is fused to the NSD3 gene in acute myeloid leukemia associated with t(8;11)(p11.2;p15). *Blood* 99(10): 3857–3860.

Sarimski K (2003). Behavioural and emotional characteristics in children with Sotos syndrome and learning disabilities. *Dev Med Child Neurol* 45(3): 172–178.

Schaefer GB, et al. (1997). The neuroimaging findings in Sotos syndrome. *Am J Med Genet* 68(4): 462–465.

Sotos JF, et al. (1964). Cerebral gigantism in childhood. A syndrome of excessively rapid growth and acromegalic features and a nonprogressive neurologic disorder. *N Engl J Med* 271: 109–116.

Stec I, et al. (1998). WHSC1, a 90 kb SET domain-containing gene, expressed in early development and homologous to a *Drosophila* dysmorphy gene maps in the Wolf-Hirschhorn syndrome critical region and is fused to IgH in t(4;14) multiple myeloma. *Hum Mol Genet* 7: 1071–1082.

Stec I, et al. (2000). The PWWP domain: a potential protein-protein interaction domain in nuclear proteins influencing differentiation? *FEBSLett* 473(1): 1–5.

Tatton-Brown K, Rahman N (2004). Clinical features of NSD1-positive Sotos syndrome. *Clin Dysmorphol* 13(4): 199–204.

Tatton-Brown K, et al. (2005a). Multiple mechanisms are implicated in the generation of 5q35 microdeletions in Sotos syndrome. *J Med Genet* 4(4): 307–313.

Tatton-Brown K, et al. (2005b). Genotype-phenotype associations in Sotos syndrome: an analysis of 266 individuals with NSD1 aberrations. *Am J Hum Genet* 77(2): 193–204.

Tei S, et al. (2006). The First Japanese Familial Sotos Syndrome with a Novel Mutation of the NSD1 Gene. *Kobe J Med Sci* 52(1): 1–8.

Tong TM, et al. (2005). Spectrum of NSD1 gene mutations in southern Chinese patients with Sotos syndrome. *Chin Med J (Engl)* 118(18): 1499–1506.

Turkmen S, et al. (2003). Mutations in NSD1 are responsible for Sotos syndrome, but are not a frequent finding in other overgrowth phenotypes. *Eur J Hum Genet* 11(11): 858–865.

van Haelst MM, et al. (2005). Familial gigantism caused by an NSD1 mutation. *Am J Med Genet A* 139(1): 40–44.

Visser R, et al. (2005a). Non-hotspot-related breakpoints of common deletions in Sotos syndrome are located within destabilised DNA regions. *J Med Genet* 42(11): e66.

Visser R, et al. (2005b). Identification of a 3.0-kb major recombination hotspot in patients with Sotos syndrome who carry a common 1.9-Mb microdeletion. *Am J Hum Genet* 76(1): 52–67.

Visser R, et al. (2006). Analysis of the NSD1 promoter region in patients with a Sotos syndrome phenotype. *J Hum Genet* 51(1): 15–20.

Waggoner DJ, et al. (2005). NSD1 analysis for Sotos syndrome: insights and perspectives from the clinical laboratory. *Genet Med* 7(8): 524–533.

Weaver DD, et al. (1974). A new overgrowth syndrome with accelerated skeletal maturation, unusual facies, and camptodactyly. *J Pediatr* 84(4): 547–552.

American Journal of Medical Genetics Part A 146A:124–127 (2008)

Research Letter

A Girl With Down Syndrome and Partial Trisomy for 21pter-q22.13:

A Clue to Narrow the Down Syndrome Critical Region

Daisuke Sato,[1,2,3] Hiroki Kawara,[4] Osamu Shimokawa,[1,3,4] Naoki Harada,[3,4] Hidefumi Tonoki,[2,5,6] Nobuhiro Takahashi,[5] Yumi Imai,[6] Hiromi Kimura,[6] Naomichi Matsumoto,[3,7] Tadashi Ariga,[2] Norio Niikawa,[1,3] and Koh-ichiro Yoshiura[1,3]*

[1]Department of Human Genetics, Nagasaki University Graduate School of Biomedical Sciences, Nagasaki, Japan
[2]Department of Pediatrics, Hokkaido University Graduate School of Medicine, Sapporo, Japan
[3]Solution Oriented Research of Science and Technology (SORST), Japan Science and Technology Agency (JST), Kawaguchi, Japan
[4]Kyushu Medical Science, Nagasaki, Japan
[5]Department of Pediatrics, Caress Alliance Medical Corporation, Tenshi Hospital, Sapporo, Japan
[6]Section of Clinical Genetics, Caress Alliance Medical Corporation, Sapporo, Japan
[7]Department of Human Genetics, Yokohama City Graduate School of Medicine, Yokohama, Japan

Received 28 January 2007; Accepted 26 May 2007

How to cite this article: Sato D, Kawara H, Shimokawa O, Harada N, Tonoki H, Takahashi N, Imai Y, Kimura H, Matsumoto N, Ariga T, Niikawa N, Yoshiura K. 2008. A girl with Down syndrome and partial trisomy for 21pter-q22.13: A clue to narrow the Down syndrome critical region. Am J Med Genet Part A 146A:124–127.

To the Editor:

Down syndrome (DS) is the most common multiple congenital anomaly syndrome with mental retardation. The majority of patients with DS have full trisomy for chromosome 21, but rare patients have partial trisomy 21, indicating the presence of a DS critical region (DSCR) that contains genes contributing to cognitive defects and/or other DS features [Antonarakis et al., 2004]. The DSCR has been narrowed down to a region within 21q22, about 5.4 Mb in length [Delabar et al., 1993; Arron et al., 2006]. Here, we describe a girl with DS and a novel karyotype that may narrow the DSCR down to 2.3 Mb.

The Japanese girl was born with a birthweight of 2,964 g (−0.3 SD), length of 46.8 cm (−1.1 SD) and OFC of 33.0 cm (mean) after 38 weeks gestation to a 22-year-old mother and a 30-year-old father. Diagnosis of DS was made soon after birth. Echocardiogram showed PDA. Although further growth was within the normal range, developmental delay was severe. Physical examinations at age 16 months showed the following abnormalities: brachycephaly with flat occiput, epicanthus, strabismus, upslanting palpebral fissures, small nose with low nasal bridge, upturned nostrils, open mouth, protruding tongue, short neck (Fig. 1a,b), short and broad hands with short fifth fingers, congenital heart defect with heart murmur, joint hyperflexibility and muscular hypotonia. These are 13 of 25 signs and satisfied the criterion for a clinical diagnosis of DS according to the Jackson score [Jackson et al., 1976].

After written informed-consent was obtained from her parents, and the study protocol was approved by the Committee for Genetic Testing and Counseling, Tenshi Hospital, cytogenetic studies were performed. A 550-band-level G-banding analysis on her metaphase chromosomes from cultured peripheral blood lymphocytes revealed an isodicentric chromosome 21, 46,XX,idic(21)(q22) (Fig. 1c). Centromere-dot (Cd) banding revealed that one side of the centromere dots of the isochromosome was separated (data not shown). This finding indicated that one of the centromeres was inactivated; hence, the isochromosome was segregating stably [Maraschio et al., 1980]. Spectral karyotyping (SKY) analysis disclosed a more complex abnormality, that is, 46,XX,t(13;21),idic(21)(q22). This karyotype was confirmed by conventional fluorescence in situ hybridization (FISH) using whole-chromosome-painting probes for chromosomes 13 and 21 (Vysis, Downers Grove, IL; Fig. 1d). Additional FISH analysis

*Correspondence to: Koh-ichiro Yoshiura, M.D., Ph.D., Department of Human Genetics, Nagasaki University Graduate School of Biomedical Sciences, Sakamoto 1-12-4, Nagasaki 852-8523, Japan.
E-mail: kyoshi@net.nagasaki-u.ac.jp

DOI 10.1002/ajmg.a.31974

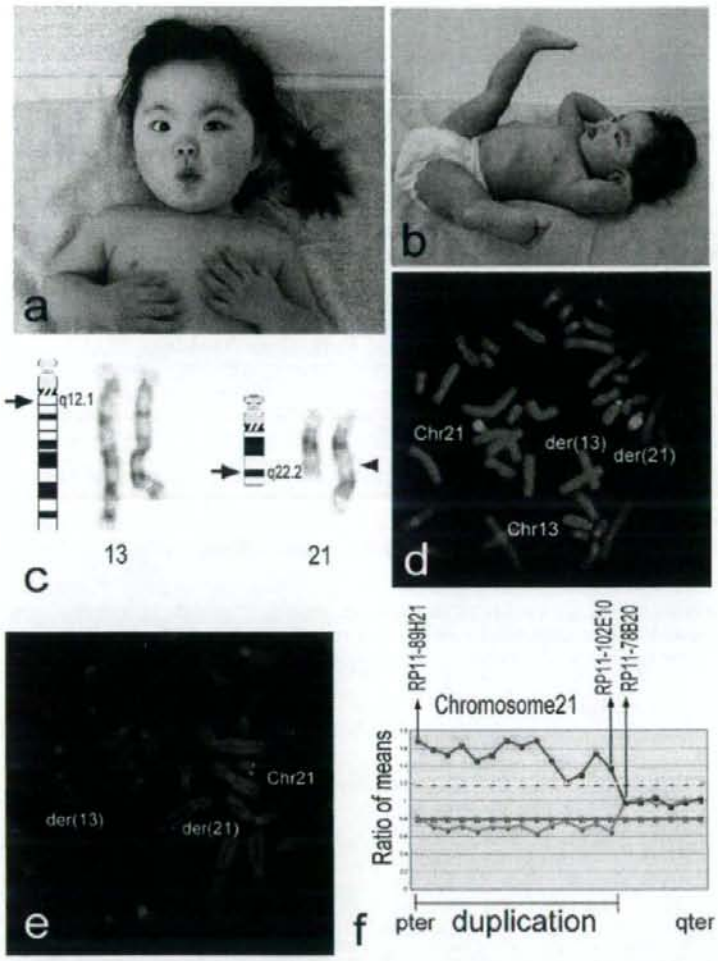

FIG. 1. **a**,**b**: The patient at age 16 months (a and b). **c**: G-banded partial karyotype of the patient. Arrows indicate the breakpoints of an inserted chromosome 13 and an isodicentric chromosome 21. **d**: FISH with chromosome-specific painting probes for chromosomes 13 (red) and 21 (green), showing an insertion of a chromosome 21-derived segment into a pericentromeric region of 13q. **e**: FISH using BAC-clone probes, RP11-1012D8 (green) and RP11-124E9 (red). Green signals appear on both der(13) and der(21) as well as normal chromosome 21, while red signals are seen on normal chromosome 21 and der(13), but not observed on der(21). **f**: Array CGH analysis demonstrates a duplication of a part of chromosome 21. The proximal and distal end clones within the duplication region were RP11-89H21 (21q11.2) and RP11-102E10 (21q22.13), respectively. The breakpoint of der (21) was suggested to be located between RP11-102E10 and RP11-78B20.

with a BAC clone (RP11-1012D8) located to 21q22.13 showed split signals both on der(13) and der(21) chromosomes as well as on normal chromosome 21. FISH using RP11-89H21 (21q11.2), RP11-166F15 (21q22.13), RP11-98O13 (21q22.13), RP11-183O20 (21q22.13), and RP11-95G19 (21q22.13) all gave signals only on both der(21) and normal chromosome 21, while signals appeared on both der(13) and normal chromosome 21 when using other BAC probes located more distantly, such as RP11-608F9 (21q22.13), RP11-749M19 (21q22.2), RP11-814F13 (21q22.3), RP11-124E9 (21q22.3), and RP11-135B17 (subtelomeric region). These analyses successfully identified the breakpoint of the isochromosome at band 21q22.13 (the UCSC genome browser, 2004 May version, http://genome.ucsc.edu/cgi-bin/hgGateway). As for the derivative chromosome 13, we could not define an insertion point precisely, because the insertion occurred closely to the centromeric region where no BAC probes were available. Within the insertion, a FISH signal for RP11-124E9 (SpectrumOrange) mapped at 21q22.3 was observed

proximally to that for RP11-1012D8 (Spectrum-Green) at 21q22.13 (Fig. 1e), demonstrating an inverted insertion on chromosome 13. All these findings indicated that the patient had partial trisomy for a 21pter-q22.13 segment, while her 21q22.13-qter region was disomic. The distal boundary of the trisomic segment lies at the region corresponding to the BAC clone, RP11-1012D8. As her parental karyotypes were normal in both Q-banding and SKY analyses, the patient's karyotype was interpreted as 46,XX,psu idic(21)(q22.13) ins(13;21)(q12.1;q22.13q22.3)dn (Fig. 2a). To know the presence of any other chromosomal aberrations, home-made whole-genome BAC-based microarray with 1.5 Mb resolution comparative genomic hybridization (array CGH) [Sato et al., 2007] was carried out using the patient's DNA. Consequently, the array CGH detected the same partial trisomy 21 (Fig. 1f), but no other deletion nor amplification in the genome.

The DSCR has always been somewhat controversial since many reports included were either premature for precise chromosome banding, include mosaic individuals, or resulted from familial translocations which may have involved undefined reciprocal deletions [Ronan et al., 2007]. Olson et al. [2004] reported that trisomy for the DSCR alone is insufficient and largely unnecessary to cause specific DS phenotypes in mice models. But, the suggestion may not be suitable for human because there are some differences between mouse and human gene content. Later, Olson et al. [2007] reported that trisomy for the DSCR is necessary for brain phenotypes of trisomic mice, thus the DSCR must have some association with the occurrence of DS. Furthermore, recent experiments using mouse models of DS suggested that a 1.5-fold increase in dosage of *DSCR1* and *DYRK1A* within the DSCR destabilizes a regulatory circuit in a cooperative way, contributing to the reduced NFATc activity and many of the characteristics of DS [Arron et al., 2006].

Interestingly, the trisomic segment of our patient partially overlaps the previously estimated DSCR at 21q22 and we have also confirmed that no known genes were disrupted at the breakpoint (Fig. 2b). With the knowledge gained from certain papers of accurately identified partial trisomy 21 that have been published in the past few years [Forster-Gibson et al., 2001; Rost et al., 2004; Kosaki et al., 2005; Kondo et al., 2006; Ronan et al., 2007], we narrow down the DSCR to a region between the proximal boundary of DS1 [Ronan et al., 2007] and the distal

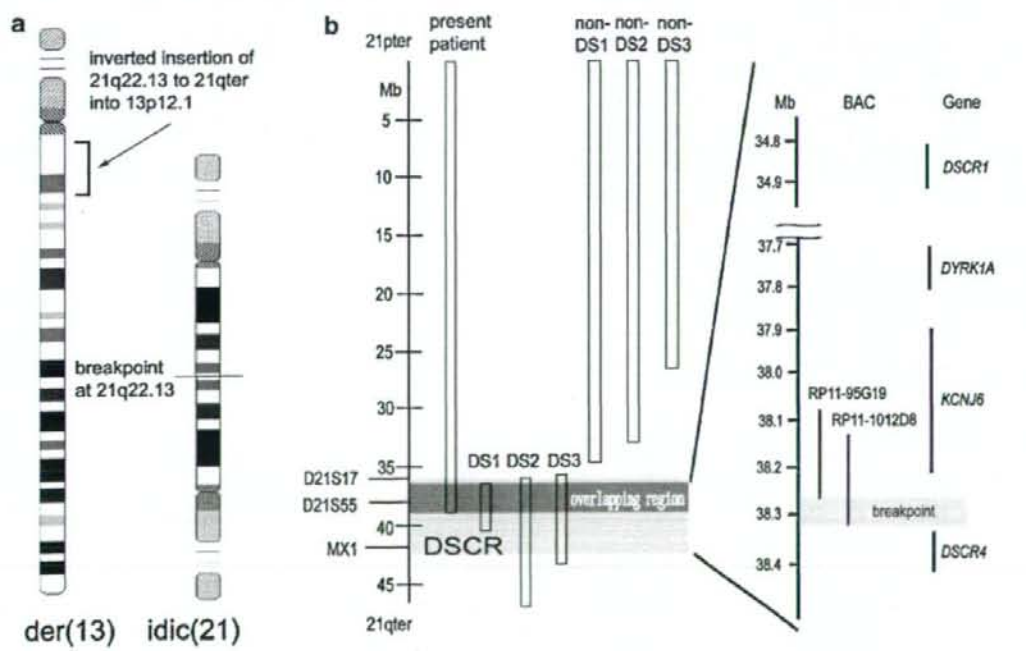

FIG. 2. **a**: Ideogram of der(13) and der(21) of the patient, showing trisomy for 21pter-q22.13 and disomy for 21q22.13-qter. **b**: Relationship between the DSCR and trisomic segments of the present DS patient and recently reported three non-DS cases; non-DS1 and DS2 [Kondo et al., 2006] and non-DS3 [Rost et al., 2004] and three other DS patients; DS1 [Ronan et al., 2007], DS2 [Forster-Gibson et al., 2001], and DS3 [Kosaki et al., 2005]. Enlargement of the overlapping region containing RP11-1012D8 with split FISH signals and its contiguous clone (RP11-95G19) without split signal. *KCNJ6* and *DSCR4* are the closest known genes flanking the breakpoint.

border of our patient, from RP11-957K9 located on 21q22.12 to RP11-1012D8 on 21q22.13, approximately 2.3 Mb in size (Fig. 2b) from the previous estimated 5.4 Mb DSCR at 21q22. [Delabar et al., 1993; Arron et al., 2006]. Since our patient manifested most of the main features of DS, we propose that the newly limited DSCR plays a role of the occurrence of DS in humans. A segment distal to the RP11-1012D8 may not attribute to the DS phenotype as far as our patient is concerned. Our data may support the studies by Arron et al. in mice. Because *DYRK1A* gene is included in the DSCR described here but *DSCR1* is not (Fig. 2b), key role of *DYRK1A* could be applied for human.

In conclusion, we have reported on a girl with DS who had a de novo 46,XX,psu idic(21)(q22.13) ins(13;21)(q12.1;q22.13q22.3) karyotype that might provide a potential clue to minimize the DSCR.

ACKNOWLEDGMENTS

Participation of the patient and her parents in this study is highly appreciated. We also thank Ms. Y. Noguchi, K. Miyazaki and A. Goto for their technical assistance.

REFERENCES

Antonarakis SE, Lyle R, Dermitzakis ET, Reymond A, Deutsch S. 2004. Chromosome 21 and Down syndrome: From genomics to pathophysiology. Nature Rev Genet 5:725–738.

Arron JR, Winslow MM, Polleri A, Chang CP, Wu H, Gao X, Neilson JR, Chen L, Heit JJ, Kim SK, Yamasaki N, Miyakawa T, Francke U, Graef IA, Crabtree GR. 2006. NFAT dysregulation by increased dosage of *DSCR1* and *DYRK1A* on chromosome 21. Nature 441:595–600.

Delabar JM, Theophile D, Rahmani Z, Chettouh Z, Blouin JL, Prieur M, Noel B, Sinet PM. 1993. Molecular mapping of twenty-four features of Down syndrome on chromosome 21. Eur J Hum Genet 1:114–124.

Forster-Gibson CJ, Davies J, MacKenzie JJ, Harrison K. 2001. Cryptic duplication of 21q in an individual with a clinical diagnosis of Down syndrome. Clin Genet 59:438–443.

Jackson JF, North ER III, Thomas JG. 1976. Clinical diagnosis of Down's syndrome. Clin Genet 9:483–487.

Kondo Y, Mizuno S, Ohara K, Nakamura T, Yamada K, Yamamori S, Hayakawa C, Ishii T, Yamada Y, Wakamatsu N. 2006. Two cases of partial trisomy 21(pter-q22.1) without the major features of Down syndrome. Am J Med Genet Part A 140A: 227–232.

Kosaki R, Kosaki K, Matsushima K, Mitsui N, Matsumoto N, Ohashi H. 2005. Refining chromosomal region critical for Down syndrome-related heart defects with a case of cryptic 21q22.2 duplication. Congenital Anomalies 45:62–64.

Maraschio P, Zuffardi O, Lo Curto F. 1980. Cd bands and centromeric function in dicentric chromosomes. Hum Genet 54:265–267.

Olson LE, Richtsmeier JT, Leszl J, Reeves RH. 2004. A chromosome 21 critical region does not cause specific Down syndrome phenotypes. Science 306:687–690.

Olson LE, Roper RJ, Sengstaken CL, Peterson EA, Aquino V, Galdzicki Z, Siarey R, Pletnikov M, Moran TH, Reeves RH. 2007. Trisomy for the Down syndrome critical region is necessary but not sufficient for brain phenotypes of trisomic mice. Hum Mol Genet 16:774–782.

Ronan A, Fagan K, Christie L, Conroy J, Nowak N, Turner G. 2007. Familial 4.3Mb duplication of 21q22 sheds new light on the Down syndrome critical region. J Med Genet 44:448–451.

Rost I, Fiegler H, Fauth C, Carr P, Bettecken T, Kraus J, Meyer C, Enders A, Wirtz A, Meitinger T, Carter NP, Speicher MR. 2004. Tetrasomy 21pter-q21.2 in a male infant without typical Down's syndrome dysmorphic features but moderate mental retardation. J Med Genet 41:e26.

Sato D, Shimokawa O, Harada N, Olsen OE, Hou JW, Muhlbauer W, Blinkenberg E, Okamoto N, Kinoshita A, Matsumoto N, Kondo S, Kishino T, Miwa N, Ariga T, Niikawa N, Yoshiura K. 2007. Congenital arhinia: Molecular-genetic analysis of five patients. Am J Med Genet Part A 143A:546–552.

CELL BIOCHEMISTRY AND FUNCTION
Cell Biochem Funct 2008; **26**: 146–150.
Published online 17 April 2007 in Wiley InterScience
(www.interscience.wiley.com) **DOI**: 10.1002/cbf.1413

Decreased serum dependence in the growth of NIH3T3 cells from the overexpression of human nuclear receptor-binding SET-domain-containing protein 1 (*NSD1*) or fission yeast su(var)3-9, enhancer-of-zeste, trithorax 2 (*SET2*)

Toshiko Yamada-Okabe [1,2*] and Naomichi Matsumoto [1]

[1] *Department of Human Genetics, Yokohama City University Graduate School of Medicine, Japan*
[2] *Department of Food Science, Faculty of Arts and Sciences, Sagami Women's University, Japan*

Nuclear receptor-binding SET-domain-containing protein 1 (*NSD1*), a culprit gene for Sotos syndrome, contains a su(var)3-9, enhancer-of-zeste, trithorax (SET) domain that is responsible for histone methyltransferase activity and other domains such as plant homeodomain (PHD) and proline-tryptophan-tryptophan-proline (PWWP) involved in protein–protein interactions in the C-terminal half of NSD1. To elucidate the function of NSD1 on cell growth, we overexpressed NSD1 in NIH3T3 cells. Cells overexpressing NSD1 grew in the presence of 2% serum, whereas vector transfected cells did not. Overexpression of the C-terminal half of NSD1 but not the N-terminal half of NSD1 also produced cell growth under low serum concentration. Furthermore, overexpression in NIH3T3 of *Schizosaccharomyces pombe* SET2 which has a SET domain but not PHD or PWWP domains conferred the reduced serum dependence. Thus, the SET domain of NSD1 is involved in cell growth by modulating serum dependence. Copyright © 2007 John Wiley & Sons, Ltd.

KEY WORDS — SET domain; histone H3K36; NSD1; SET2; serum

INTRODUCTION

Nuclear receptor-binding SET domain protein 1 (*NSD1*) is the gene responsible for Sotos syndrome[1] which is characterized by rapid growth in childhood, distinctive craniofacial features including macrocephaly, and mental retardation. NSD1 protein contains a su(var)3-9, enhancer-of-zeste, trithorax (SET) domain and other functional domains including plant homeodomain (PHD) and proline-tryptophan-tryptophan-proline (PWWP) domains, both of which are involved in protein–protein interaction.[2] Most enzymes with histone methyltransferase activity contain a SET domain, and therefore, it has been considered that NSD1 also has histone methyltransferase activity. In fact, the recombinant protein-containing SET domain of NSD1 was demonstrated to have the ability to methylate lysine 36 of histone H3 and lysine 20 of histone H4.[3] Embryos of NSD1-deficient mice showed apoptosis at E7.5–E8.0, indicating that NSD1 protein is essential for gastrulation and development in mice. However, the physiological role of NSD1 remains to be elucidated.

In order to gain more insight into the physiological role of NSD1, we constitutively expressed it in NIH3T3 cells. We found that NIH3T3 cells expressing NSD1 were able to proliferate even under the condition of a low serum concentration, and that the C-terminal region containing the SET domain of NSD1 was essential for the decreased serum dependence. Similar results were obtained from the expression of *Schizosaccharomyces pombe* (*S. pombe*) SET2 which contains a SET domain but not a PWWP or PHD domain. The results indicate that the SET domain of NSD1 positively regulates cell growth.

* Correspondence to: T. Yamada-Okabe, Department of Food Science, Faculty of Arts and Sciences, Sagami Women's University, 2-1-1 Bunkyo, Sagamihara, Kanagawa 228-8533, Japan. Tel/Fax: +81-42-742-1945. E-mail: t-okabe@star.sagami-wu.ac.jp

Received 3 January 2007
Revised 14 February 2007
Accepted 22 February 2007

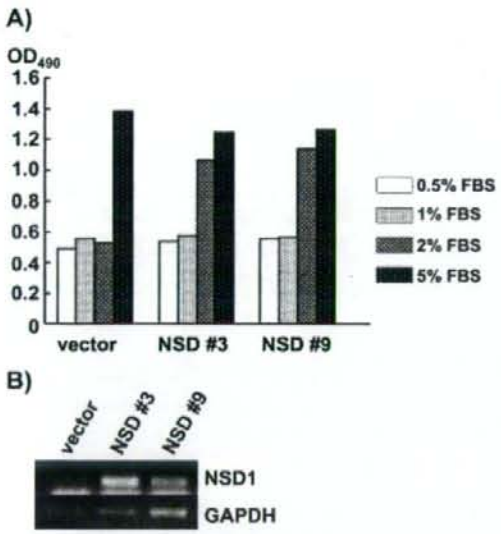

Figure 1. Reduced serum dependence from the constitutive expression of *NSD1* in NIH3T3 cells. (A) One thousand cells per well were plated on 96-well microplates and were cultured in the absence or presence of 0.5, 1, or 2% FBS. After 14 days, 20 μL of CellTiter 96 AQ_{ueous} One Solution Reagent was added to the cells, and the cells were further incubated for 3 h. Absorbance at 490 nm, which correlates with the viable cell number, is shown. The two independent clones which overexpressed NSD1 in NIH3T3 cells were designated NSD#3 and NSD#9. (B) Expression of *NSD1* was confirmed by RT-PCR. The obtained PCR products were analyzed by agarose gel electrophoresis

MATERIALS AND METHODS

Isolation of S. pombe SET2-related gene

Genomic DNA of *S. pombe* was prepared from the L972 strain as described.[4] *S. pombe* cells were treated with zymolyase to disrupt the cell wall, and the resulting spheroplasts were lysed by 1% SDS. After digesting RNA with 0.1 mg ml^{-1} RNaseA at 37 °C for 1 h, genomic DNAs were precipitated by ethanol. The *S. pombe* SET2 gene was cloned by PCR using a set of primers, 5′-GAGCCCGGGATGCAGACGGCATCA-TCTCT-3′ and 5′-GAGCCCGGGTTAAGCAGCTTT-TTTCGGGG-3′. Human NSD1 cDNA and *S. pombe* SET2 were cloned at the *Sca*I site of pCruz-His (Santa Cruz Biotechnology, Inc., CA) and the *Eco*RV site of pCruz-His (Santa Cruz), respectively, to drive human NSD1 cDNA and *S. pombe* SET2 transcription from the CMV promoter. NIH3T3 cells were transfected with pCruz-His (Santa Cruz) or pCMV-Tag4 (Stratagene, CA, USA) carrying the human NSD1 cDNA or *S. pombe* SET2 by Lipofectamine™ (Invitrogen, CA, USA). After selection with 0.5–1 mg ml^{-1} G418 for 2 weeks, G418-resistant clones which expressed NSD1 or SET2 were selected and used for the experiments.

GenBank accession numbers for human NSD1 and *S. pombe* SET2 are AF395588 and NM001020411, respectively.

Cell proliferation assay

Cells (1.5×10^3) of NIH3T3 expressing or not expressing human NSD1 or *S. pombe* SET2 were cultured in 100 μL of medium in the absence or presence of 0.5, 1, 2, or 5% of fetal bovine serum at 37 °C for at least 7 days. The vector-transfected NIH3T3 cells were used as the control. At the end of the culture, 20 μL of CellTiter 96 AQ_{ueous} One Solution Reagent (Promega, WI, USA) containing 5-(3-carboxymethoxyphenyl)-2-(4, 5-dimenthylthiazoly)-3-(4-sulfophenyl) tetrazolium salt (MTS) was added to the medium, and the cells were incubated at 37 °C for 1–4 h. Absorbance at 490 nm, which represents the amount of formazan product and thereby viable cell number, was measured using a microplate reader (BioRad, CA, USA).

RT-PCR

One microgram of total RNA was used for single-stranded cDNA synthesis. After reverse-transcriptase reaction, the cDNA was amplified by 25 cycles of consecutive incubations at 94 °C for 30 s, 60 °C for 30 s, and 72 °C for 60 s with primers for the indicated cDNA and RNA LA PCR kit (AMV) Ver 1.1 (Takara, Shiga, Japan).

The primer sequences for PCR were 5′-CCCAG-GATGGATCAGACCTGTGAAC-3′, 5′-AGCAGAC-CCATTTAAATACTCTAC-3′, 5′-TATTTGTGGACT-CACCAAGCCCGAGTCTTC-3′, and 5′-TGCAGTG-AAGATCTGTACCCTGCC-3′ for *NSD1*, and 5′-GA-GCCCGGGATGCAGACGGCATCATCTCT-3′ and 5′-TTTCTTTTCGGTTAAGAAAACATCCACCTT-3′ for *S. pombe SET2*.

RESULTS AND CONCLUSIONS

Effects of overexpression of NSD1 on cell growth

Sotos syndrome, accompanied by rapid growth in childhood, is caused by haploinsufficiency of *NSD1*.[1] Therefore, we asked whether *NSD1* is involved in cell growth under certain circumstances. Therefore, *NSD1* was expressed constitutively in NIH3T3 under the CMV promoter (Figure 1B). Constitutive expression

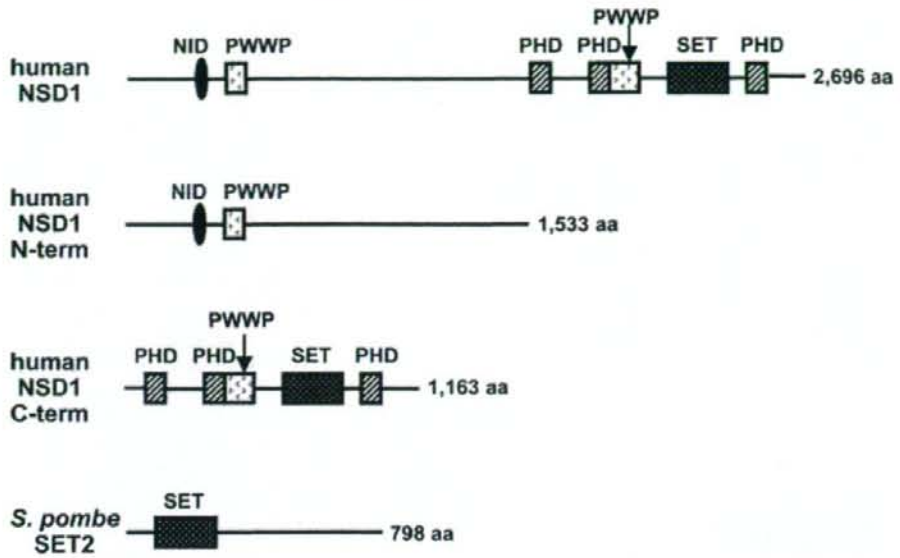

Figure 2. Domain structures of total human NSD1, N- and C-terminal halves of NSD1, and *S. pombe* SET2

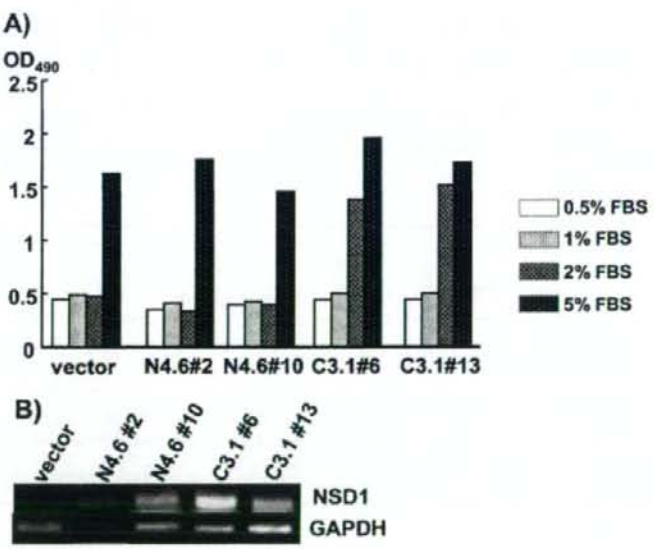

Figure 3. Reduced serum dependence from the constitutive expression of the C-terminal half of NSD1 in NIH3T3 cells. (A) One thousand cells per well were plated on 96-well microplates and were cultured in the absence or presence of 0.5, 1, or 2% FBS. After 14 days, 20 μL of CellTiter 96 AQ_{ueous} One Solution Reagent was added to the cells, and the cells were further incubated for 3 h. Absorbance at 490 nm, which correlates with the viable cell number, is shown. The independent clones which overexpressed in the N-terminal half and in the C-terminal half of NSD1 in NIH3T3 cells were designated N4.6#2 and N4.6#10 and C3.1#6 and C3.1#10, respectively. (B) Expression of *NSD1* mRNA fragments in the N-terminal half or the C-terminal half of *NSD1* was confirmed by RT-PCR. The obtained PCR products were analyzed by agarose gel electrophoresis

DOI: 10.1002/cbf

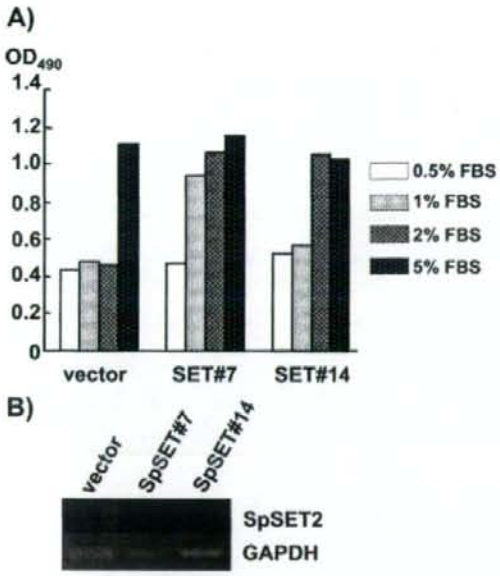

Figure 4. Reduced serum dependence from the constitutive expression of *S. pombe* SET2 in NIH3T3 cells. (A) One thousand cells per well were plated on 96-well microplates and were cultured in the absence or presence of 0.5, 1, or 2% FBS. After 14 days, 20 μL of CellTiter 96 AQ_{ueous} One Solution Reagent was added to the cells, and the cells were further incubated for 3 h. Absorbance at 490 nm, which correlates with the viable cell number, is shown. The two independent clones which overexpressed SET2 in NIH3T3 cells were designated SET#7 and SET#14. (B) Expression of the *SET2* mRNA was confirmed by RT-PCR. The obtained PCR products were analyzed by agarose gel electrophoresis

of NSD1 did not affect the growth of the cells when the cells were cultured with 10% FBS. However, cells expressing NSD1 were able to proliferate even in 2% serum, whereas the vector-transfected cells did not grow in such a low concentration of serum, as indicated by the results from two independent clones, #3 and #9, compared to the control (Figure 1A).

SET domain was necessary for decreased serum dependence

NSD1 contains a nuclear receptor interacting domain (NID) in the N-terminal half, 2 PWWP domains (1 in each half), 3 PHD domains in the C-terminal half, and a SET domain in the C-terminal half (Figure 2). Translocation of the NSD1 gene to the NUP98 locus, t(5;11)(q35;p15.5), causes childhood acute myeloid leukemia,[5] and the SET domain has been considered to be involved in the cell cycle. We examined whether the C-terminal half of NSD1 affects cell proliferation. The results show that decreased serum dependence was reproduced by the constitutive expression of the C-terminal half of NSD1, as indicated by a comparison of independent clones C3.1#6 and C3.1#13 with the control, but not by the N-terminal half, as indicated by a comparison of independent clones N4.6#2 and N4.6#10 with the control (Figure 3A).

S. pombe SET2 has a SET domain but no other domains present in NSD1 (Figure 2). To further confirm that the decreased serum dependence is largely attributable to the function of the SET domain, we constitutively expressed the *S. pombe* SET2 gene in NIH3T3 cells and found that the cells expressing *S. pombe* SET2 also grew in 2% serum, indicated by the comparison of clones #7 and #14 with the control (Figure 4A).

The SET domain of NSD1 methylates lysine 36 of histone H3 and lysine 20 of histone H4 *in vitro*,[3] whereas the *S. pombe* Set2 protein methylates only lysine 36 of histone H3.[6] Because the constitutive expression of *S. pombe* SET2 decreased the serum dependence of NIH3T3, the ability to methylate lysine 36 of histone H3 seems to be important for a decrease of serum dependence in cell growth. Yeast *Saccharomyces cerevisiae* and *S. pombe* Set2 proteins have been reported to be associated with the hyperphosphorylated form of RNA polymerase II,[6–9] and thus methylation of lysine 36 of histone H3 may be related to transcriptional activation. It has been reported that histone H3 modification with phosphorylation and acetylation correlates with the cell cycle.[10] Furthermore, methylation of lysine 36 in histone H3 is necessary for normal development in *Neurospora crassa*[11] and prevention of early flowering in *Arabidopsis thaliana*.[12] On the other hand, methylation of lysine 20 of histone H4 has been found in heterochromatin,[13] which implies that methylation of lysine 20 of histone H4 may cause transcriptional repression. It may be of interest to clarify whether methylation activity of lysine 20 of histone H4 is also necessary for the stimulation of growth in low concentrations of serum.

ACKNOWLEDGEMENTS

This work was supported in part by a grant-in-aid from the Ministry of Education, Culture, Sports, Science and Technology of Japan to NM.

REFERENCES

1. Kurotaki N, Imaizumi K, Harada N, *et al*. Haploinsufficiency of NSD1 causes Sotos syndrome. *Nat Genet* 2002; **30**: 365–366.
2. Kurotaki N, Harada N, Yoshiura K, Sugano S, Niikawa N, Matsumoto N. Molecular characterization of NSD1, a human homologue of the mouse Nsd1 gene. *Gene* 2001; **279**: 197–204.
3. Rayasam GV, Wendling O, Angrand P-O, *et al*. NSD1 is essential for early post-implantation development and has a catalytically active SET domain. *EMBO J* 2003; **22**: 3153–3163.
4. Hoffman SC. 1997; Preparation of yeast DNA. In *Current Protocols in Molecular Biology*, Ausubel FM, Brent R, Kingston RE, Moore DD, Seidman JG, Struhl K (eds). John Wiley and Sons: 13.11.1–13.11.4.
5. Brown J, Jawad M, Twigg SRF, *et al*. Acryptic t(5;11)(q35;p15.5) in 2 children with acute myeloid leukemia with apparently normal karyotypes, identified by a multiplex fluorescence *in situ* hybridization telomere assay. *Blood* 2002; **99**: 2526–2531.
6. Morris SA, Shibata Y, Noma K, *et al*. Histone H3 K36 methylation is associated with transcription elongation in *Schizosaccharomyces pombe*. *Eukaryot Cell* 2005; **4**: 1446–1454.
7. Strahl BD, Grant PA, Briggs SD, *et al*. Set2 is a nucleosomal histone H3-selective methyltransferase that mediated transcriptional repression. *Mol Cell Biol* 2002; **22**: 1298–1306.
8. Schaft D, Roguev A, Kotovic KM, *et al*. The histone 3 lysine 36 methyltransferase, SET2, is involved in transcriptional elongation. *Nucl Acids Res* 2003; **31**: 2475–2482.
9. Kizer KO, Phatnani HP, Shibata Y, Hall H, Greenleaf AL, Strahl BD. A novel domain in set2 mediates RNA polymerase II interaction and couples histone H3 K36 methylation with transcript elongation. *Mol Cell Biol* 2005; **25**: 3305–3316.
10. McManus KJ, Hendzel MJ. The relationship between histone H3 phosphorylation and acetylation throughout the mammalian cell cycle. *Biochem Cell Biol* 2006; **84**: 640–657.
11. Adhvaryu KK, Morris SA, Strahl BD, Selker EU. Methylation of histone H3 lysine 36 is required for normal development in *Neurospora crassa*. *Eukaryot Cell* 2005; **4**: 1455–1464.
12. Zhao Z, Yu Y, Meyer D, Wu C, Shen W-H. Prevention of early flowering by expression of FLOWERING LOCUS C requires methylation of histone H3 K36. *Nat Cell Biol* 2005; **7**: 1256–1260.
13. Shotta G, Lachner M, Marma K, *et al*. A Silencing pathway to induce H3-K9 and H4-K20 trimethylation at constitutive heterochromatin. *Genes Dev* 2004; **18**: 1251–1262.

American Journal of Medical Genetics Part A 146A:1241–1247 (2008)

Two New Cases of Pure 1q Terminal Deletion Presenting With Brain Malformations

Yoko Hiraki,[1]* Nobuhiko Okamoto,[2] Tomoko Ida,[3] Yusei Nakata,[4] Masahiro Kamada,[5] Yonehiro Kanemura,[6] Mami Yamasaki,[6] Hiroko Fujita,[7] Gen Nishimura,[8] Mitsuhiro Kato,[9] Naoki Harada,[3,10] and Naomichi Matsumoto[10,11]

[1]Hiroshima Municipal Center for Child Health and Development, Hiroshima, Japan
[2]Osaka Medical Center and Research Institute for Maternal and Child Health, Osaka, Japan
[3]Department of Molecular Cytogenetics, Kyushu Medical Science, Inc., Nagasaki, Japan
[4]Medical Center for Premature and Neonatal Infants, Hiroshima City Hospital, Hiroshima, Japan
[5]Division of Pediatrics, Hiroshima City Hospital, Hiroshima, Japan
[6]Institute for Clinical Research and Department of Neurosurgery, Osaka National Hospital, Osaka, Japan
[7]Research Department, Mitsubishi Kagaku Bio-Clinical Laboratories, Tokyo, Japan
[8]Division of Radiology, Tokyo Metropolitan Kiyose Children's Hospital, Kiyose, Japan
[9]Department of Pediatrics, Yamagata University School of Medicine, Yamagata, Japan
[10]Solution-Oriented Research for Science and Technology, Japan Science and Technology Agency, Tokyo, Japan
[11]Department of Human Genetics, Yokohama City University Graduate School of Medicine, Yokohama, Japan

Received 25 July 2007; Accepted 15 December 2007

We describe two new cases of pure 1q terminal deletions. BAC FISH analysis precisely defined the size of deletions. The first is a girl with 10.3-Mb deletion showed typical features of 1q43 deletion as well as a simplified gyral pattern, which was rarely found in 1q43 deletion. The other boy also presented with most of 1q43 deletion features but several atypical symptoms were noted including hydrocephalus, adducted thumbs, and flexion restriction of proximal interphalangeal joints in left hand. A concomitant novel missense mutation in *L1CAM* was identified in addition to 11.5-Mb deletion. Reviewing all the cases of pure 1q terminal deletion in the literature suggests that it is a clinically recognizable syndrome. © 2008 Wiley-Liss, Inc.

Key words: 1q terminal deletion; brain malformation; X-linked hydrocephalus; *L1CAM* mutation

How to cite this article: Hiraki Y, Okamoto N, Ida T, Nakata Y, Kamada M, Kanemura Y, Yamasaki M, Fujita H, Nishimura G, Kato M, Harada N, Matsumoto N. 2008. Two new cases of pure 1q terminal deletion presenting with brain malformations. Am J Med Genet Part A 146A:1241–1247.

INTRODUCTION

Since the first report of Mankinen et al. [1976], more than 50 deletions at 1q42-qter and uninvolved with other chromosomal abnormalities have been documented [Gentile et al., 2003; van Bever et al., 2005; Boland et al., 2007; Hill et al., 2007; Merritt et al., 2007]. These deletions may result in a recognizable phenotype including characteristic facial appearance, microcephaly, psychomotor retardation, and variable other anomalies [van Bever et al., 2005]. Most deletions were only cytogenetically examined, but detailed molecular mapping information is available in 14 cases [Gentile et al., 2003; van Bever et al., 2005; Kanemoto et al., 2006; Boland et al., 2007; Hill et al., 2007; Merritt et al., 2007; Poot et al., 2007].

Here we report on two new cases of pure 1q43-qter deletion with brain abnormalities, a simplified gyral pattern previously reported in two cases [Hill et al., 2007] and hydrocephalus. Deletions were precisely mapped by FISH analysis. Clinical features of pure 1q distal deletion from all the reported patients are summarized. Finally the hydrocephalus, which was

Grant sponsor: Ministry of Health, Labour and Welfare, Japan; Grant sponsor: JST.

*Correspondence to: Yoko Hiraki, M.D., Hiroshima Municipal Center for Child Health and Development, Hikarimachi 2-15-55, Higashi-Ku, Hiroshima 732-0052, Japan.
E-mail: hy-772v@enjoy.ne.jp
**Correspondence to: Naomichi Matsumoto, M.D., Ph.D., Department of Human Genetics, Yokohama City University Graduate School of Medicine, Fukuura 3-9, Kanazawa-ku, Yokohama 236-0004, Japan.
E-mail: naomat@yokohama-cu.ac.jp

DOI 10.1002/ajmg.a.32275

rare in 1q terminal deletion, turned out to be caused by a concomitant *L1CAM* mutation.

METHODS AND RESULTS

Subjects

Patient 1. The 5-year-old girl is the second product of an unrelated 31-year-old mother and 32-year-old father. She was born by cesarean at 38 weeks of gestation due to intrauterine growth retardation. Her birth weight was 2,190 g (−2.3 SD), length 40 cm (−4.6 SD), and OFC 30 cm (−2.1 SD). Multiple malformations included incomplete cleft palate, hemivertebra, talipes valgus, and tetralogy of Fallot (TOF) which was surgically repaired at her age of 1 year. At 15 months, she was referred to us for evaluation of her developmental delay. She had microcephaly (−4.4 SD), prominent metopic suture, sparse and fine hair, round face, thin and bow-shaped eyebrows, strabismus, upslanting palpebral fissures, periorbital fullness, hypertelorism, epicanthus, flat nasal bridge, short and broad nose, hypoplastic nares, smooth and long philtrum, thin vermilion borders, well formed "cupid's" bow, mouth with downturned corners, tucked in lower lip, micro/retrognathia, incomplete cleft palate, prominent antihelices, ear lobe clefts, left retroauricular fold, and short neck (Fig. 1A and Table I). Additionally, she had abnormal hands and feet consisting of small, edematous dorsum of hands and feet, tapering fingers, bilateral singular palmar creases, bilateral vertical tali, proximally placed 2nd toes, and scoliosis and bilateral accessory nipples were noticed. She was diagnosed as an autistic disorder, based on the DSM-IV. Autonomic dysfunctions were observed, such as gastric esophageal reflux (GER), deglutition abnormalities, abnormal sweating, flushing spells, peripheral coldness, and apneic spell. Her dysphagia with GER was treated during 1–3 years. At 2 years, her weight was 7,700 g (−3.0 SD), length 71.2 cm (−4.0 SD), and OFC 39.5 cm (−4.9 SD). Complex partial seizure requiring anticonvulsant treatment started at her 2 years, was deteriorated by influenza encephalopathy, leading to severe developmental delay at 5 years (DQ = 9). At age of 5 years, her weight was 11.8 kg (−2.4 SD), length 89.5 cm (−3.9 SD), and OFC 42.0 cm (−4.6 SD). She could sit alone and creep, but could not recognize her parents. Uncontrollable seizures and autonomic dysfunction persisted. She also had hypoplastic labia majora and minora. Stiff barrel-shaped thorax was also recognized. Brain magnetic resonance imaging (MRI) revealed microcephaly with a simplified gyral pattern, thin corpus callosum, and reduced white-matter volume (Fig. 1A). Echocardiography confirmed no other abnormalities. 1q distal deletion was suspected as she presented with growth and psychomotor retardation, typical craniofacial features, abnormal hands and feet, and other anomalies.

Patient 2. He was 5 years old and the first child of an unrelated 39-year-old mother and 48-year-old father. The mother had one spontaneous abortion at 7 weeks of gestation. In pregnancy, IUGR, large ventricles of fetal brain, and hydramnios were noted at the third trimester, and fetal karyotype was normal after fetal blood sampling. He was born by cesarean at 36 weeks. His birth weight was 1,242 g (−3.9 SD), length 39 cm (−3.1 SD), and OFC 27.6 cm (−2.9 SD).

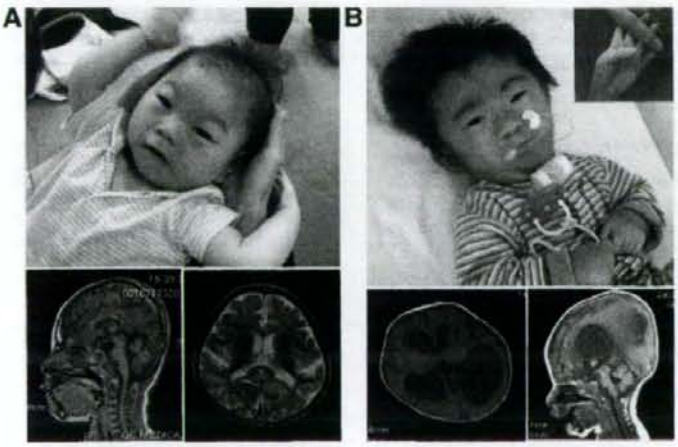

FIG. 1. **A**: Patient 1. Face at 19 months (upper), and MRI images at 5 years (lower left, sagital section; lower right, horizontal). Typical facial appearance of 1q distal deletion is seen. A simplified gyral pattern and thin corpus callosum were noted. **B**: Patient 2. Face at 19 months (upper) along with left hand, and MRI at 4 years (lower left, horizontal section; lower right, sagittal). Midface hypoplasia, bushy hair, and synophrys were recognized, which is rarely seen. Adducted thumb was demonstrated. MRI shows large massa intermedia and marked dilation of the lateral ventricles. Thin corpus callosum, stenosis of the Sylvius aqueduct, and mild pontocerebellar atrophy are observed.

TABLE I. Clinical Findings of Pure Type of Del(1q) Syndrome

Clinical features	Previously reported patients					Our patients	
	Pure type of 1q deletion (n = 53) M/F=20:33	1q42deletion (n = 22) M/F = 9:13	1q43deletion (n = 17) M/F = 3:14	1q44deletion (n = 6) M/F = 3:3	Interstitial deletion of 1q42--44 (n = 8) M/F = 5:3	Case 1	Case 2
General							
Growth retardation	37/42[a]	14/16	14/14	5/5	4/7	+	+
Psychomotor retardation	48/50	20/20	17/17	6/6	5/7	+	+
CNS anomalies	35/39	10/13	14/15	5/5	6/6	+	+
Agenesis/thin corpus callosum	26/28	6/8	11/11	4/4	5/5	+	+
Hydrocephalus	2/2	1/1	1/1	0/0	0/0	−	+
Communicating type	1/2	1/1	0/1	0/0	0/0	−	−
Non-communicating type	1/2	0/1	1/1	0/0	0/0	−	+
Hypotonia	25/28	13/15	8/8	3/4	1/1	+	+
Seizures	33/39	11/15	16/16	4/6	2/2	+	+
Autonomic dysfunction	18/18	9/9	6/6	3/3	0/0	+	+
Dysphagia/feeding difficulties	12/12	6/6	5/5	1/1	0/0	+	+
Craniofacial							
Microcephaly	41/47	18/20	15/17	5/6	3/4	+	−
Prominent metopic suture/trigonocephaly	9/14	5/7	2/4	2/3	0/0	+	−
Sparse, fine hair	10/12	6/7	2/2	1/2	1/1	+	−
Round face	16/16	10/10	2/2	2/2	2/2	+	−
Upslanting palpebral fissures	23/27	12/15	7/7	3/4	1/1	+	+
Epicanthic folds	32/34	18/19	11/12	2/2	1/1	+	−
Impression of hypertelorism	14/17	8/9	4/5	2/2	0/1	+	+
Vision, eye anomaly	18/20	11/11	4/5	2/2	1/2	+	+
Strabismus	14/20	9/13	2/3	2/3	1/2	+	+
Short, broad nose/flat nasal bridge	37/37	19/19	12/12	5/5	1/1	+	+
Smooth, long philtrum	14/17	9/11	2/3	2/2	1/1	+	+
Thin vermillion borders	20/21	11/12	6/6	3/3	0/0	+	+
Well formed "cupid's" bow	9/10	6/7	2/2	1/1	0/0	+	−
Downturned corners of the mouth	29/32	15/17	11/11	2/3	1/1	+	+
Micro/retrognathia	28/35	16/19	7/10	2/3	3/3	+	+
Abnormal palate	20/25	12/14	4/5	1/3	3/3	+	+
Low set/dysplastic ears	30/38	14/19	7/7	5/5	4/7	+	+
Short/webbed neck	29/33	15/16	10/11	3/4	1/2	+	+
Extremities							
Abnormal hands	19/33	12/15	4/11	2/4	1/3	+	+
Clinodactyly of the 5th fingers	7/14	5/9	2/4	0/0	0/1	−	−
Hypoplastic fingernails	4/13	3/9	0/2	1/1	0/1	−	−
Small hands	4/11	3/7	0/2	0/0	1/2	+	+
Tapering fingers	4/11	1/5	1/3	2/2	0/1	+	−
Shortened thumbs	3/10	3/7	0/2	0/0	0/1	−	−
Syndactyly	3/10	1/5	2/4	0/0	0/1	−	−
Polydactyly	2/9	1/5	1/3	0/0	0/1	−	−
Adducted thumbs	0/0	0/0	0/0	0/0	0/0	−	+
Flexion restriction of PIP joints	0/0	0/0	0/0	0/0	0/0	−	+
Abnormal feet	20/29	7/12	9/10	4/5	0/2	+	+
Urogenital							
Genital anomalies (male, female)	18/18, 5/11	9/9, 2/4	3/3, 3/6	2/2, 0/0	4/4, 0/1	+	+
Kidney/urine pathway anomalies	6/15	0/6	4/6	1/1	1/2	−	+

(*Continued*)

TABLE I. (*Continued*)

Clinical features	Previously reported patients					Our patients	
	Pure type of 1q deletion (n = 53) M/F=20:33	1q42deletion (n = 22) M/F = 9:13	1q43deletion (n = 17) M/F = 3:14	1q44deletion (n = 6) M/F = 3:3	Interstitial deletion of 1q42–44 (n = 8) M/F = 5:3	Case 1	Case 2
Others							
Cardiac anomalies	18/37	9/18	4/12	3/3	2/4	+	+
Ventricular septal defect	13/13	7/7	4/4	1/1	1/1	−	+
Noncompaction of left ventricular myocardium	1/1	0/0	0/0	0/0	1/1	−	+
Skeletal anomalies	18/23	5/8	10/11	1/1	2/3	+	+
Dysspondylism	8/12	3/6	4/5	0/0	1/1	+	+

[a]Number of patients having the feature/number of patients examined as to the feature. (These data are referred to Hum Genet 41:115–120, 1978; Jpn J Hum Genet 39:433–437, 1994; Am J Hum Genet 81:292–304, 2007; J Med Genet 38:175–178, 2001; Hum Genet 48:151–156, 1979; J Med Genet 25:211–212, 1988; Am J Med Genet A 117:251–254, 2003; Am J Med Genet 35:379–382, 1990; Am J Med Genet 80:396–398, 1998; Ann Genet 35:167–169, 1992; Am J Med Genet 22:685–694, 1985; Ann Genet 31:193–194, 1988; Hum Genet 42:333–337, 1978; Birth Defects Orig Artic Ser 12:131–136, 1976; Am J Med Genet 25:599–600, 1986; Am J Med Genet 28:371–376, 1987; Am J Med Genet A 143:599–603, 2007; Am J Ep Pediatr 11:729–732, 1978; Ann Genet 27:178–179, 1984; Am J Med Genet 40:488–492, 1991; Ann Genet 25:154–155, 1982; Ugeskr Laeger 143:2500–2502, 1981; Am J Med Genet A 138:68–69, 2005; Ann Genet 30:126–128, 1987; Am J Med Genet A 128:352–363, 2004; Am J Med Genet 98:103–106, 2001; Eur J Pediatr 155:720, 1996; Ann Genet 28:177–180, 1985; Clin Genet 35:289–292, 1989; Ann Genet 26:161–164, 1983; Am J Med Genet A 135:91–95, 2005; Am J Med Genet 24:1–6, 1986; Pediatrics 77:786, 1986; Acta Paediatr Jpn 30:696–702, 1988; Clin Genet 19:544–545, 1981; Eur J Med Genet 49:247–253, 2006.)

Multiple malformations were recognized including hydrocephalus, ventricular septal defect (VSD), left hydronephrosis, and hypospadias. A shunt operation for ventriculomegaly was not performed. Developmental delay was noticed soon after birth. At age of 6 months, he received tracheostomy because of prolonged respiratory distress, as well as orchidopexy and bilateral inguinal herniotomy. VSD was repaired at 1 year and his development was then evaluated. He could not control his head with hypotonia. Severe psychomotor delay, growth retardation and serious dysphagia were recognized. Facial features included macro/brachycephaly, bushy hair, midface hypoplasia, thick and bow shaped eyebrows, upslanting palpebral fissures, periorbital fullness, hypertelorism, flat nasal bridge, short and broad nose, hypoplastic alae nasi, smooth and long philtrum, thin vermilion borders, downturned corners of the mouth, tucked in lower lip, micrognathia, high arched palate, low-set ears, prominent antihelices, involuted and sticked helices, webbed neck and posterior low hair line (Fig. 1B and Table I). Other multiple abnormalities included barrel-shaped thorax, widely spaced nipples, hypospadias, abnormally placed anus, abnormal hands and feet consisting of bilateral single transverse creases, small and edematous hands and feet, an adducted left thumb and severe restriction of PIP joints of a left hand and overlapping of the 1st toes over the 2nd toes (Fig. 1B). Abnormal eye movement, GER, butterfly vertebra of T4, and scoliosis were recognized. At age of 18 months, his weight was 6,380 g (−3.7 SD), length 68.5 cm (−3.5 SD), and OFC 46.5 cm (−0.9 SD). His DQ at $3^4/_{12}$ years was scored as 15. At age of 5 years, his weight was 13.6 kg (−1.6 SD), length 94.0 cm (−2.9 SD) and OFC 52.0 cm (+0.75 SD). He could take away towels covering his favorite toys, but he could not control his head with hypotonia, or recognize his parents. Tube feedings were required. Occasional burst of laughter and supraversion of his eyeballs were observed without any paroxysmal discharge. Delayed bone age (≤2 SD) were noticed. At age of $5^4/_{12}$ years, he had repeated bleeding from the orifice of tracheostomy. Embolotherapy of left subclavian artery collateral vessels was performed to prevent bleedings and cardiac ultrasonography revealed noncompaction of the left ventricular myocardium (NCLVM). Brain MRI revealed obstructive hydrocephalus associated with stenosis of aqueduct and marked dilation of lateral ventricles as well as large massa intermedia, thin corpus callosum, and mild pontocerebellar atrophy (Fig. 1B). Moderate left sensorineural hearing loss was noted. Left hydronephrosis with normal renal function was gradually ameliorated.

Genetic Analyses

G-banded chromosomal analysis of peripheral blood leukocytes indicated that both karyotypes of

Patients 1 and 2 were del(1)(q43) (Fig. 2 A,B). Fluorescence in situ hybridization (FISH) analysis using all chromosomal subtelomeric clones [Vysis ToTelVysion™ Multicolor FISH probe panel VYS-33-270000 (Abbott, Tokyo, Japan)] documented that both were a pure type of 1q terminal deletion as no other subtelomeric clones did show any abnormalities. Detailed FISH using BACs mapped to 1q42-1qter was performed as previously described [Shimokawa et al., 2005]. Deletions in Patients 1 and 2 were 10.3 Mb (from RP11-201D24 to 1q telomere) and 11.5 Mb (from RP11-1078D23 to telomere) in size, respectively (Fig. 2C). Parental chromosomes of both patients were normal. Since macro/brachycephaly, hydrocephalus and adducted left thumb in Patient 2, were not reported in 1q distal deletion and might be associated with L1-associated diseases, *L1CAM* was tested. Using genomic DNA from peripheral leukocytes as a template, all *L1CAM* exons were amplified by PCR, purified and subsequently sequenced using the BigDye Terminator Cycle Sequencing kit (Applied Biosystems, Foster City, CA). A novel missense mutation (c.92T → C: p.Val31Ala) in exon 3 was identified, and his mother was a heterozygous carrier (Fig. 3). Father was not tested. P.Val31 is evolutionally conserved through mammals and we sequenced more than 200 alleles and observed the same base pair change in another affected patient, but never in other patients or family members through the study of LI-associated diseases (data not shown). Thus we concluded that the nucleotide change was pathogenic.

DISCUSSION

Deletion from the 1q telomere is now proposed as a specific clinical syndrome [van Bever et al., 2005]. We have summarized clinical features of 53 cases of pure 1q distal deletions with reasonable clinical description (Table I). Among these, 22 patients were described as 1q42-qter deletion, 17 with 1q43-qter deletion, 6 with 1q44-qter deletion and 8 with interstitial deletion around 1q42-q44 [Mankinen et al., 1976; Gentile et al., 2003; van Bever et al., 2005; Kanemoto et al., 2006; Boland et al., 2007; Hill et al., 2007; Merritt et al., 2007]. We could successfully extract common clinical features of 1q distal deletions such as growth and psychomotor retardation, hypotonia, seizure, autonomic dysfunction, microcephaly, agenesis of corpus callosum possibly associated with *AKT3* haploinsufficiency [Boland et al., 2007], specific facial features, abnormal hands/

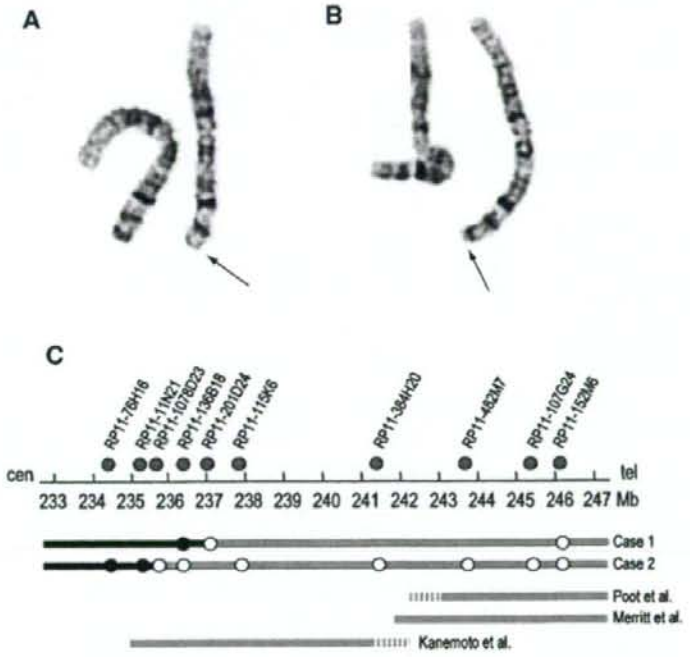

FIG. 2. Partial karyotype of Patients 1 (**A**) and 2 (**B**) and schematic presentation of 1q43-qter deletions (**C**). A,B: Arrow indicates deletion. C: Above the genomic scale, position of BAC clones was indicated as gray circle. Thick gray lines indicate deletion while black intact. White and black circles are BAC clones mapped to deleted and intact regions, respectively. Minimal critical regions for the 1q terminal deletion syndrome [Merritt et al., 2007; Poot et al., 2007] as well as an interstitial deletion associated with the noncompaction of left ventricular myocardium [Kanemoto et al., 2006] are depicted.

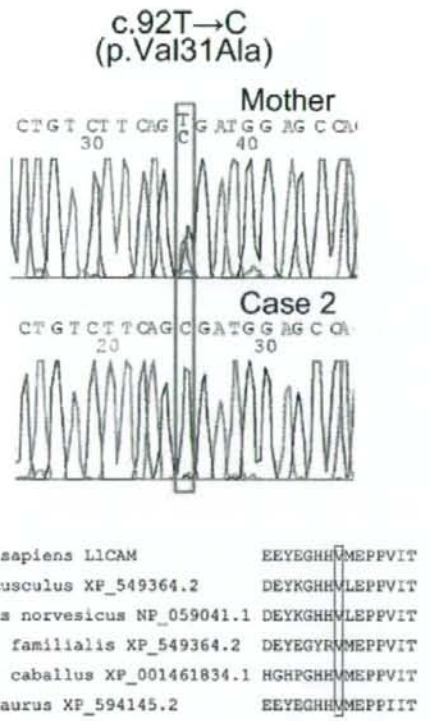

FIG. 3. A missense mutation, c.92T → C (p.Val31Ala) at exon 3 of *L1CAM* in Patient 2 (lower) and his mother (upper). Clustal W demonstrated that p.Val31 is evolutionally conserved through mammals (CLUSTALW ver. 1.83: http://clustalw.ddbj.nig.ac.jp/top-j.html). [Color figure can be viewed in the online issue, which is available at www.interscience.wiley.com.].

feet, and urogenital anomalies. Using this summary, we could propose that Patient 1 presented with a typical phenotype of 1q distal deletion. A simplified gyral pattern of brain was recently described in two cases [Hill et al., 2007], which may be due to abnormal neuronal and glial proliferation [Barkovich, 2005] and could be causative for uncontrollable seizures.

In Patient 2, several atypical conditions such as hydrocephalus, sensorineural hearing loss, left adducted thumb and restricted flexion of PIP joints were noticed in addition to many representative features of 1q distal deletion. Hydrocephalus associated with aqueductus stenosis, adducted left thumb, and mother's miscarriage history prompted us to test *L1CAM* for X-linked hydrocephalus (XLH). As expected, a novel missense mutation was identified. To our best knowledge, this is the first case of 1q distal deletion with accompanying XLH. The mutation was also recognized heterozygously in the mother. On the contrary, 1q distal deletion occurred as de novo. The *L1CAM* mutation (p.Val31Ala) in exon 3 is located at a signal peptide domain, which exists as an extracellular N-terminal region. P.Val31 is evolutionally conserved and the nucleotide change was recognized in another affected patient with an L1-associated disease. It belongs to class II mutations (amino acid substitutions in the extracellular part of L1 protein), raging from severe to mild phenotypes of L1-assosiated diseases [Yamasaki et al., 1997; Kanemura et al., 2006]. The NCLVM found in Patient 2 and another [Kanemoto et al., 2006] is intriguing. The overlapping 6.4-Mb region of the two deletions may harbor a gene(s) for the rare heart phenotype (Fig. 2C). Fetal blood karyotype by conventional chromosomal analysis was normal. When some brain malformations are recognized at ultrasound evaluation in prenatal periods, molecular techniques such as subtelomeric FISH/array CHG are encouraged in order to detect abnormal submicroscopic chromosomal changes.

In conclusion, two new cases of 1q43-qter deletions are described, who present with brain malformations: a simplified gyral pattern in Patient 1 and hydrocephalus with aqueductus stenosis in Patient 2. Each deletion was cytogenetically visible, precisely mapped by FISH, and was much larger than a 4.9–5.4-Mb minimal critical region (10.3 Mb and 11.5 Mb in size) (Fig. 2) [Merritt et al., 2007; Poot et al., 2007]. It may be challenging to delineate the phenotype/genotype correlation for pure 1q terminal deletion as most of deletions contain the minimal critical region for the syndrome. The simplified gyral pattern is reported as in the 3rd case. The hydrocephalus and other atypical features led to identification of a concomitant *L1CAM* mutation, being the first report in association with 1q distal deletion. Finally, the NCLVM associated with 1q terminal deletion found in this study is unique, while NCLUM has been observed in other chromosome conditions; this is the first report in 1q terminal deletion. This observation may be useful for narrowing down a disease locus.

ACKNOWLEDGMENTS

We are grateful to Dr. R. Kawamura and the staff of the rehabilitation institution 'Futaba En' for handicapped children, who have given habilitation and education to our patients. In addition, we thank Mr. Y. Unesaki, the physical therapist who provided beneficial information to us. This study was supported by Research Grant from the Ministry of Health, Labour and Welfare (N. M.) and SORST from JST (N.M.).

REFERENCES

Barkovich AJ. 2005. Pediatric neuroimaging. 4th edition. Philadelphia: Lippincott Williams & Wilkins. pp 329–332.

Boland E, Clayton-Smith J, Woo VG, McKee S, Manson FDC, Medne L, Zackai E, Swanson EA, Fitzpatrick D, Millen KJ, Sherr EH, Dobyns WB, Black GCM. 2007. Mapping of deletion and translocation breakpoints in 1q44 implicates the serine/

threonine kinase AKT3 in postnatal microcephaly and agenesis of the corpus callosum. Am J Hum Genet 81:292–304.

Gentile M, Di Carlo A, Volpe P, Pansini A, Nanna P, Valenzano MC, Buonadonna AL. 2003. FISH and cytogenetic characterization of a terminal chromosome 1q deletion: Clinical case report and phenotypic implications. Am J Med Genet Part A 117A:251–254.

Hill AD, Chang BS, Hill RS, Garraway LA, Bodell A, Sellers WR, Walsh CA. 2007. A 2-Mb critical region implicated in the microcephaly associated with terminal 1q deletion syndrome. Am J Med Genet Part A 143A:1692–1698.

Kanemoto N, Horigome H, Nakayama J, Ichida F, Xing Y, Buonadonna AL, Kanemoto K, Gentile M. 2006. Interstitial 1q43-q43 deletion with left ventricular noncompaction myocardium. Eur J Med Genet 49:247–253.

Kanemura Y, Okamoto N, Sakamoto H, Shofuda T, Kamiguchi H, Yamasaki M. 2006. Molecular mechanisms and neuroimaging criteria for severe L1 syndrome with X-linked hydrocephalus. J Neurosurg 105:403–412.

Mankinen CB, Sears JW, Alvarez VR. 1976. Terminal (1)(q43) long-arm deletion of chromosome no. 1 in a three-year-old female. Birth Defects Orig Artic Ser 12:131–136.

Merritt JL II, Zou Y, Jalal SM, Michels VV. 2007. Delineation of the cryptic 1qter deletion phenotype. Am J Med Genet Part A 143A:599–603.

Poot M, Kroes HY, SE VDW, Eleveld MJ, Rooms L, Nievelstein RA, Olde Weghuis D, Vreuls RC, Hageman G, Kooy F, Hochstenbach R. 2007. Dandy-Walker complex in a boy with a 5 Mb deletion of region 1q44 due to a paternal t(1;20)(q44;q13.33). Am J Med Genet Part A 143A:1038–1044.

Shimokawa O, Miyake N, Yoshimura T, Sosonkina N, Harada N, Mizuguchi T, Kondoh S, Kishino T, Ohta T, Remco V, Takashima T, Kinoshita A, Yoshiura K, Niikawa N, Matsumoto N. 2005. Molecular characterization of del(8)(p23.1p23.1) in a case of congenital diaphragmatic hernia. Am J Med Genet Part A 136A:49–51.

van Bever Y, Rooms L, Laridon A, Reyniers E, van Luijk R, Scheers S, Wauters J, Kooy RF. 2005. Clinical report of a pure subtelomeric 1qter deletion in a boy with mental retardation and multiple anomalies adds further evidence for a specific phenotype. Am J Med Genet Part A 135A:91–95.

Yamasaki M, Thompson P, Lemmon V. 1997. CRASH syndrome: Mutations in L1CAM correlate with severity of the disease. Neuropediatrics 28:175–178.